Geo-Mar Lett (2013) 33:311–318
DOI 10.1007/s00367-013-0333-3

ORIGINAL

The Queen Charlotte Fault, British Columbia: seafloor anatomy of a transform fault and its influence on sediment processes

J. Vaughn Barrie · Kim W. Conway · Peter T. Harris

Received: 5 February 2013 / Accepted: 29 May 2013 / Published online: 9 June 2013

Abstract The Queen Charlotte Fault Zone (QCFZ) off western Canada is the northern equivalent to the San Andreas Fault Zone, the Pacific–North American plate boundary. Geomorphologic expression and surface processes associated with the QCFZ system have been revealed in unprecedented detail by recent seabed mapping surveys. Convergence of the Pacific and North American plates along northern British Columbia is well known, but how the QCFZ accommodates this convergence is still a subject of controversy. The multibeam sonar bathymetry data reveal, for the first time, evidence of a fault valley with small depressions on the upper slope, offshore central Haida Gwaii (Queen Charlotte Islands). The depressions form where strike-slip right-step offsets have realigned the fault due to oblique convergence. Core stratigraphy and radiocarbon dating of sediments within the fault valley and small depressions suggest that these features are recent in origin. In addition, the development of the fault valley and dislocation of submarine canyons control sediment migration from the continental shelf through to the lower slope. This interpretation of the geomorphic expression of major plate tectonic processes along the QCFZ can now be tested with new surveys subsequent to the October 2012 magnitude 7.7 earthquake.

J. V. Barrie (✉) · K. W. Conway
Natural Resources Canada, Geological Survey of Canada–Pacific, Institute of Ocean Sciences, P.O. Box 6000, Sidney, British Columbia V8L 4B2, Canada
e-mail: vbarrie@nrcan.gc.ca

P. T. Harris
Geoscience Australia, G.P.O. Box 378, Canberra, ACT 2601, Australia

Introduction

The Queen Charlotte Fault (QCFZ) extends for over 350 km along the western margin of British Columbia offshore of the Haida Gwaii (Queen Charlotte Islands) archipelago (Fig. 1). Along with numerous small events, two dozen large earthquakes have occurred this century along the fault zone (Rogers 1986), with the largest (magnitude 8.1) occurring adjacent to the north-western edge of the continental shelf of Haida Gwaii in 1949 (Fig. 1), and the most recent on 27 October 2012 (magnitude 7.7). Bostwick (1984) estimated a horizontal rupture length of the 1949 earthquake to be 490 km (300 km north and 190 km south of the epicentre) with an average coseismic displacement of 4.0–7.5 m. A continued rise in earthquake hazard for Haida Gwaii is anticipated, based on stress distribution (Bufe 2005).

The QCFZ is the northern part of the complex and poorly understood transition from subduction between the Juan de Fuca and North American plates in the Cascadia margin to a right-slip transform between the Pacific and North American plates. Two competing theories involve either one or more microplates being subducted south of the QCFZ, or a new strike-slip fault system accommodating Pacific–North America motion in a region of distributed shear offshore (Rohr and Tryon 2010).

The QCFZ extends northwards as the Fairweather Fault Zone for over 1,300 km into southern Alaska as far as the northern Gulf of Alaska, and is longer than the San Andreas Fault system with 75% of the fault offshore (Plafker et al. 1978; Carlson et al. 1988). Along the southern portion of the QCFZ, ~20° oblique convergence becomes purely strike-slip towards the north with a change in margin trend (Hyndman and Hamilton 1993). Two models have been proposed to describe

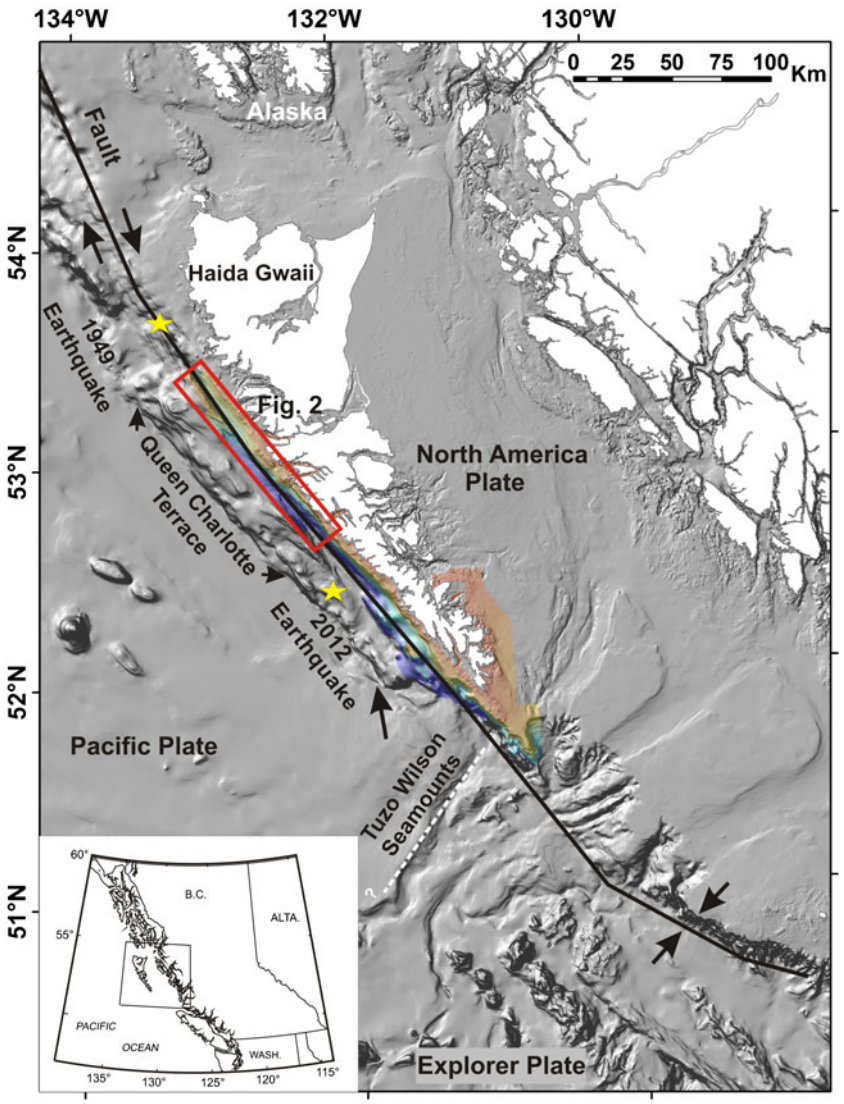

Fig. 1 Map showing the location of the Queen Charlotte Fault Zone in the plate tectonic setting of western Canada. Also shown are the locations of the 1949 8.1 and the 2012 7.7 magnitude earthquakes, the completed area of multibeam sonar mapping and Fig. 2

this convergence of the Pacific and North American plates along Haida Gwaii (Mazzotti et al. 2003): internal shortening (Rohr et al. 2000) and underthrusting of the Pacific Plate at a greater depth (Smith et al. 1993; Bustin et al. 2007). Seawards of the fault a narrow marginal plateau, the Queen Charlotte Terrace (Fig. 1), is a prism consisting of a melange of deformed marine sediments and basalt which have accreted to the margin as a result of the oblique convergence (Prims et al. 1997).

The QCFZ is near vertical and seismically active down to ~21 km (Hyndman and Ellis 1981), with mainly right-lateral transform motion of approx. 50–60 mm/year (Prims et al. 1997; Rohr et al. 2000). Motion along the fault system has deformed and fractured bedrock and basement rocks of the region (Rohr et al. 2000). From the Tuzo Wilson Seamounts (Fig. 1) to Alaska, the two plates are similar in mechanical properties (Rohr et al. 2000) and they both deform internally. Response to regional rapid sea-level changes during the end of the last glaciation (Barrie and Conway 2002; Hetherington and Barrie 2004) further indicate that the two plates are elastically independent (Rohr et al. 2000). This decoupling of the North American Plate along the fault enabled the Queen Charlotte Basin to behave like a hinge in response to glacial unloading (Hetherington and Barrie 2004).

Recently collected multibeam swath bathymetry has revealed the geomorphology and surface processes associated with the QCFZ in unprecedented detail. Considerable understanding of the fault system has been derived from geophysical and seismic analyses, but fully three-dimensional high-resolution multibeam sonar imagery of this marine fault has never been published. The objective of this study is to interpret this imagery to identify seabed processes associated with active tectonic boundaries and determine if the surface expression of the active fault provides insight to support either of the two proposed models of plate boundary convergence. Understanding processes related to tectonics of the QCFZ have implications for other transpressive areas, such as California and Anatolia (e.g. Arrowsmith and

Zielke 2009; Johnson and Watt 2012; Gökaşan et al. 2012; İşcan et al. 2013).

Materials and methods

Multibeam swath bathymetry was acquired off the west coast of Haida Gwaii between 2009 and 2010 using a hull-mounted Kongsberg EM710 system which operates at a frequency of 70 to 100 kHz (Fig. 1). In addition, continuous hull-mounted Knudson Chirp 3260 sub-bottom profiles were acquired in conjunction with the multibeam data collection. The surveys were carried out from the *CCGS Vector* by the Canadian Hydrographic Service, in cooperation with the Geological Survey of Canada. The tracks were positioned so as to insonify 100% of the seafloor with 50 to 100% overlap. Positioning was accomplished with broadcast differential GPS, and the multibeam data were corrected for sound velocity variations in the stratified water column using sound speed casts. The data were edited for spurious bathymetric and navigational points and subsequently processed using CARIS software. The gridded data were exported as ASCII files and imported into ArcInfo software for processing and image production. Multibeam swath images formed the interpretive framework for delineation of surface processes along the fault.

Based on this interpretation two areas were further investigated with the collection of seabed photographs and sediment samples in July 2011 aboard the *CCGS John P. Tully*. A Geological Survey of Canada deep-water digital 35 mm camera system was used to collect seabed photographs along transects crossing the fault valley, and piston cores were collected from targeted features along the same transects. In the laboratory, cores were split, photographed and sampled for textural analyses and radiocarbon dating. Grain size descriptions based on core sub-samples adhere to the Wentworth size class scheme for clastic sediments (Wentworth 1922). AMS radiocarbon dates were undertaken on shells collected within the cores and analysed by Beta Analytic Inc.

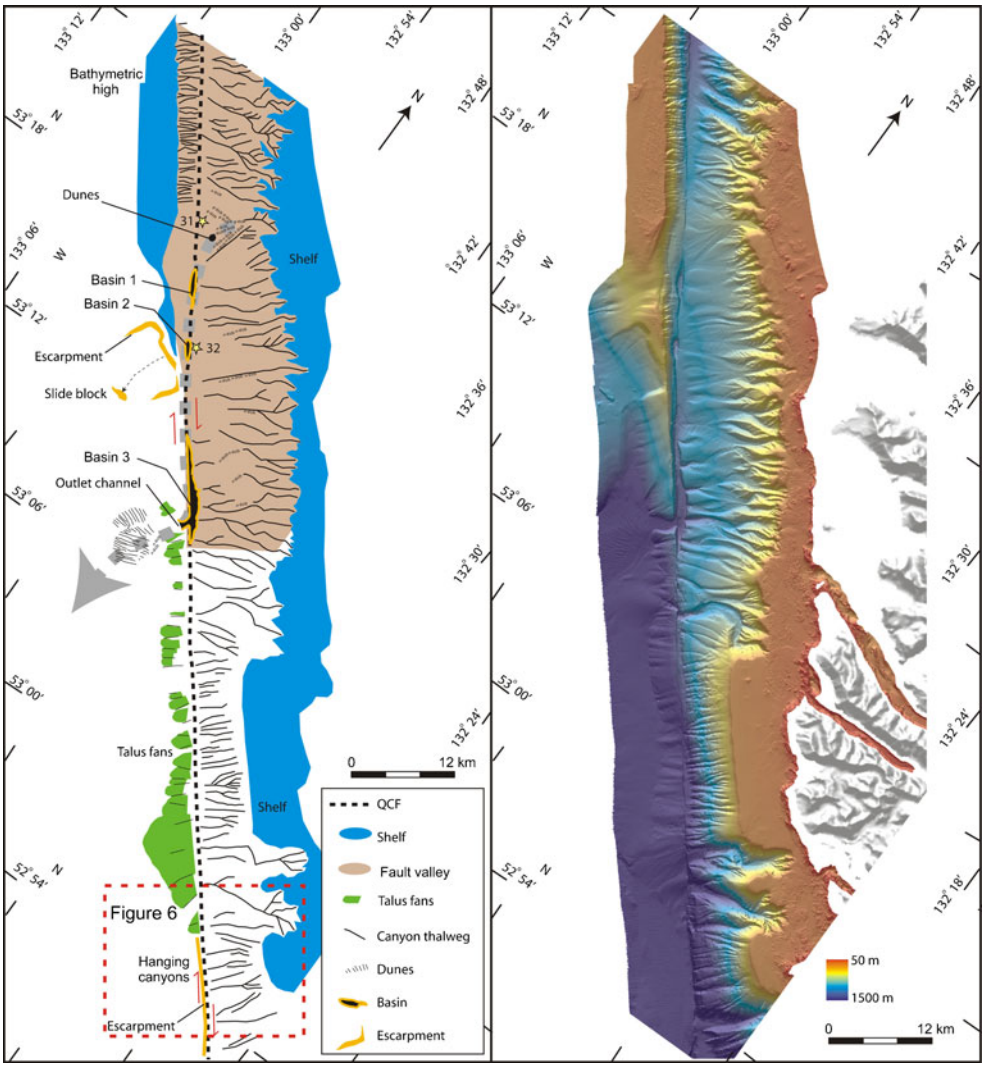

Fig. 2 Multibeam sonar map showing an 80 km long segment of the QCFZ lineation and right-step morphology. Basin 1 has a mean depth of 790 m and the surrounding fault scarp has heights ranging from 60–80 m. The floor of basin 2 has a mean depth of 840 m and the surrounding fault scarp has a height of about 100 m. Basin 3 has a gently southward sloping floor, with a mean depth of 860–960 m. *Arrow* Inferred transport pathway for sediments in transit downslope, which appear to bypass the fault valley, exiting through a narrow outlet channel which feeds into a large dune field. *Stars* Locations of bottom photographs (Fig. 5) and sediment cores (Fig. 4)

Results

The QCFZ is clearly visible as a very recent feature in multibeam sonar data, manifest as a sharp linear feature located within a ~3 km wide shelf valley which has maximum depths ranging from 600 to 1,000 m (the fault valley; Fig. 2). On the seaward side of the fault valley the seafloor rises to form a relatively flat shelf-like fragment up to 4.5 km wide and extending for more than 28 km. The fragment forms a detached mesa-like platform, oval shaped in plan view with a mean water depth of about 180 m, which is the same as the adjacent outer continental shelf, but separated from the shelf by the fault valley by about 6 km (Fig. 3). Off this fragment a large slide block has moved approx. 6 km downslope from its interpreted point of origin (Figs. 2 and 3).

Submarine canyons occur both on the remnant fragment and the landward flank of the fault valley (Fig. 3, inset A), but appear to be more gently sloping, more widely spaced and more deeply incised into the landward than the seaward flank of the fault valley (cf. closely spaced canyons incising the offshore fragment dip landwards into the fault valley; Fig. 2). Several of the largest canyons on the landward valley flank incise and head at the shelf break.

Along the axis of the fault valley are small geomorphic basins (depressions; Figs. 2 and 3). The basins are elongate depressions, oval in shape. Basin 1 is 500 m wide and 1,800 m in length, basin 2 300 m wide and 1,400 m in length, and basin 3 up to 700 m wide and 7,500 m in length. The three basins form flat-floored sections of the fault valley floor, having mean depths of 760 to 960 m, and they are generally surrounded by 60–200 m high fault scarps. Between the basins the fault valley is floored by an irregular surface. The fault scarp itself shifts 250 to 300 m to the east (right-step offset) as it enters and leaves basins 1 and 2. For example, the fault trace in basin 1 can be seen entering on the western side of the southern end of the basin and it exits on the eastern side of the basin on the northern end (Fig. 3). However, the fault trace shows no evidence of shifting (right-stepping) through basin 3. The mean depth of the fault valley through the three basins continues to increase towards the south, whereas the shelf and seaward bathymetric high remain at the same depth (Fig. 2).

A sediment core was collected from the fault valley north of basin 1 (31 in Fig. 2) and another core was collected within basin 2 (32 in Fig. 2). Core 31 within the fault valley contained fine sand over sandy gravels; core 32 within basin 2 recovered 3.4 m of turbidites and debris flow deposits (Fig. 4). Radiocarbon data from a shell and shell fragments from two locations separated by 111 cm in core 31 dated closely to 14,300 ^{14}C BP; a single shell in core 32 dated to 40,000 ^{14}C BP (Table 1).

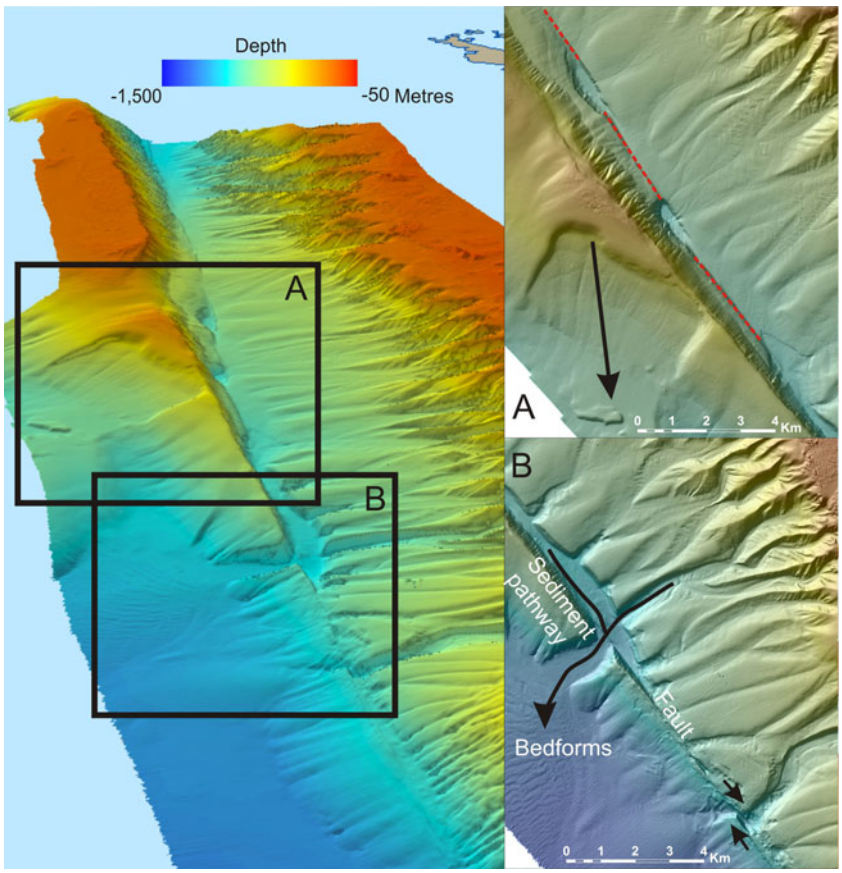

Fig. 3 Three-dimensional image illustrating the morphology of the QCFZ. Highlights include the flat-topped fragment, basins resulting from fault right-stepping offsets, submarine failure (inset A), 600 m of canyon displacement along fault, and sediment pathway and migrating sedimentary bedforms moving out of the fault valley (inset B). *Arrows* in the bottom right of inset B indicate the submarine canyon displacement along the fault

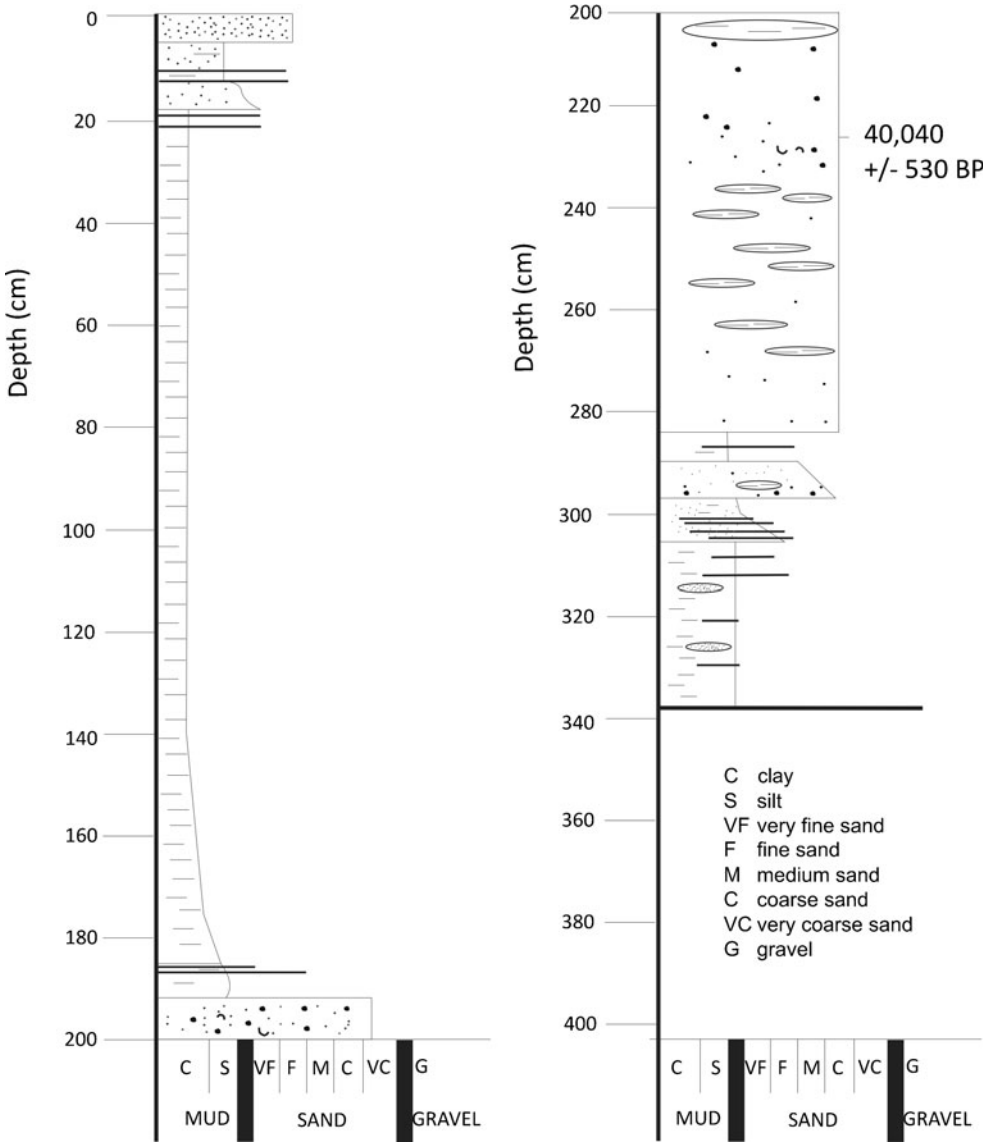

Fig. 4 Stratigraphy of piston core 32 (cf. Fig. 2) collected in basin 2 within the fault valley. Notice the turbidity units between 1.9 and 3.2 m

Underwater photographs at the fault scarp exhibit rock outcrops with evidence of recent deformation. Indications of deformation include the upturned and blocky, angular fabric of mudstone outcrops (Fig. 5a) as well as mudstone bedding planes which are exposed in outcrop along vertical scarps (Fig. 5b). The fissile gray mudstone is thinly covered in a dark olive-coloured, foraminifer-rich, 2–3 mm thick veneer which is normally bioturbated.

South of the fault valley the trend of the QCFZ is expressed by a narrow ledge or bench feature. Submarine canyons incise the slope on the landward side of the ledge, whereas talus fans are developed on the seaward side (Fig. 2). Further south the ledge gives way to an escarpment, on the seaward side of which talus fans are absent and valley thalwegs are raised above the level fault valley floor, forming hanging canyons. Bedforms located in the canyons occur

Table 1 Radiocarbon dates from sediment cores. Core 31 is located in the fault valley at 612 m water depth and core 32 in basin 2 at 849 m water depth (Fig. 2)

Core	Sample depth	Material dated	Lab. no.	Radiocarbon age	Corrected age
Core 31	144 cm	Shell fragments	Beta-333043	14,700±60	14,290±60
Core 31	255 cm	Shell	Beta-333044	14,000±60	14,400±60
Core 32	228 cm	Shell	Beta-333045	40,410±530	40,040±530

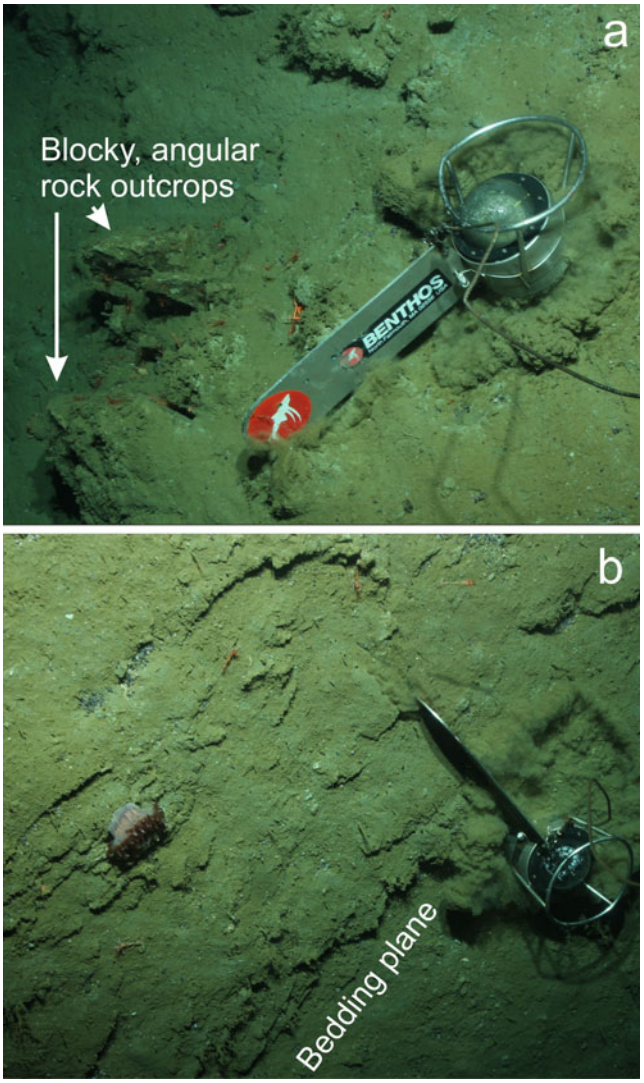

Fig. 5 Bottom photographs (stn 32, cf. Fig. 2: 53°14.87′N, 132°54.47′W, 780 m water depth) taken where the QCFZ breaks the seafloor. **a** Photo showing deformation of mudstone outcrops including the upturned and blocky fabric; **b** photo showing mudstone bedding planes which are exposed in outcrop along the nearly vertical scarp. Length of compass fin is 30 cm; compass dome is ~8 cm across

with their crests oriented sub-normal to canyon thalwegs (Fig. 6).

Discussion

The convergence of the QCFZ results in right-stepping offsets forming small depressions (grabens, down-dropped block) along the northern part of the fault valley. The transfer of slip of the active fault trace can be seen in the shift to the east in basins 1 and 2. The presence of right-steps is a feature of the Hosgri strike-slip fault, one of the major faults of the transform plate boundary along California (Hanson et al. 2004; Johnson and Watt 2012). Here right-steps from 200 to 1,000 m produce localized extensional or contractional deformation along the fault (Hanson et al. 2004). The Hosgri Fault Zone is a component of a large linear system of right-stepping faults which extend for more than 400 km (Hanson et al. 2004). Similarly, the QCFZ realigns by en echelon right-step offsets or pull-aparts resulting in subsiding basins (grabens) up to 700 m in length. Compressive left-steps have also been imaged on GLORIA data further north along the QCFZ (Rohr et al. 2000). Basin 3, however, does not exhibit an obvious right-step offset and could be an oblique branch of faulting (negative flower structure) forming a sag pond.

The bathymetric high, seaward of the fault valley, has the morphologic appearance of a flat-topped remnant fragment of the margin (Figs. 2 and 3). Lateral motion along the fault zone could have moved the fragment north, though the mechanism which would have allowed for separation outwards from the continental shelf is not obvious. Another possibility is that the fragment may also be uplifted compressively deformed sediments from the Pacific Plate (Rohr et al. 2000) or a combination of both processes. Seismic data are needed to determine the origin of these bathymetric highs and to test if either of these hypotheses is possible. The fragment would have been eroded during early Holocene sea-level lowstand, when sea levels could have been as low as 180 m below present day (Barrie and Conway 2002; Hetherington and Barrie 2004), further masking the origin.

The narrow fault valley broadens south of 52°58′N (Fig. 2) at which point the fault trace marks the edge of hanging canyons along the upper slope, landwards of the fault (Fig. 6). Hanging submarine canyons normally occur as tributaries of larger canyon systems in which greater rates of erosion in the main thalweg leave tributary thalwegs stranded, hanging above the level of the main canyon floor (Shepard 1949; Greene et al. 2002). In this study a different mechanism, vertical and lateral displacement along a fault, is responsible for the creation of hanging canyons. Although hanging canyons are normally associated with glacial erosion processes (e.g. in fjords), they can also result from tectonism, such as tributary canyons of the Monterey Canyon system (Greene et al. 2002).

In the present paper, identification of right-stepping offsets in part supports internal shortening as proposed by Rohr et al. (2000) to accommodate the convergence off central Haida Gwaii. The 1949 M 8.1 earthquake, just north of the area in Fig. 2, displayed a right-lateral first motion and occurred along the fault valley, supporting a primarily strike-slip motion. However, at the southern extreme of the QCFZ, accommodation of the greater convergence may be due to underthrusting of the Pacific Plate as suggested by Smith et al. (1993) and Bustin et al. (2007). Initial results suggest that the 27 October 2012 magnitude 7.7 earthquake (Fig. 1) was an oblique subduction event (Szelica 2013), similar to the Cascadian subduction zone to the south of the QCFZ.

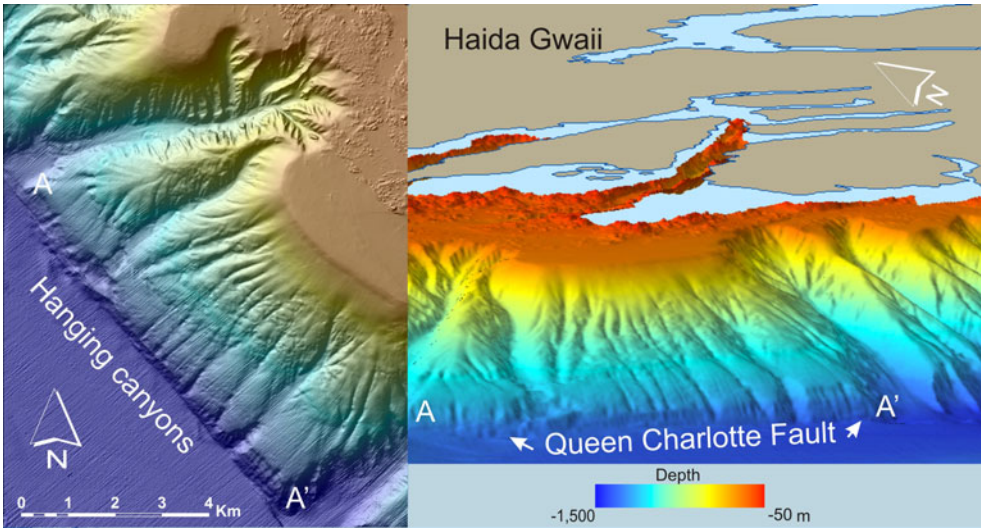

Fig. 6 Multibeam sonar bathymetry three-dimensional imagery showing hanging submarine canyons cut by the QCFZ. For location of image, see Fig. 2

Surface processes

In the present study area, the continental slope exhibits evidence of mass wasting and turbidity flows, such as the large slide block which has moved southwards seawards of the fault valley (Figs. 2 and 3) and debris fields located at the downslope terminus of several submarine canyons. Turbidites and debris flow deposits occur within the fault valley (Fig. 4). Radiocarbon dates (Table 1) suggest that sediments in the fault valley date to initial deglaciation, when sea level was much lower (Barrie and Conway 1999), and those in basin 2 predate the last glaciation (Blaise et al. 1990). The present-day Haida Gwaii continental shelf is primarily bedrock and little to no sediment reaches the shelf from the island archipelago. The lack of glacial deposits in the fault valley and small basins suggest that the basins may be of recent origin. Relict sediments are being moved through the fault valley, likely derived from deposits further upslope within the submarine canyons.

Bottom photographs taken from the basins show they are characterized by rock outcrops and sessile fauna (Fig. 5b). It therefore appears that sediments are bypassing the fault valley and exiting to the south via an outlet channel at 1,100 m water depth and forming into subaqueous dunes 5 m in height with wavelengths of 300 m (Figs. 2 and 3, inset B). The outlet channel is located on the seaward side of the fault and probably formed in relation to a large submarine canyon located further south, and was subsequently transported to its present location.

Conclusions

Multibeam imagery provides new evidence for right-step offsets which realign the transpressive strike-slip QCFZ off central Haida Gwaii. The development of small pull-apart basins would appear to support an ongoing internal shortening style of deformation at the plate boundary. In addition, the data reveal that the resultant fault valley and basin morphology has altered the sediment pathways downslope. Specifically, submarine canyon mouths have been shifted, thereby altering the transport of sediment into the fault valley and out along a major channel onto the lower slope.

Acknowledgments Multibeam bathymetry was collected by the Canadian Hydrographic Service in cooperation with the Geological Survey of Canada. This paper was supported in part by a collaborative agreement between Geoscience Australia and the Geological Survey of Canada (GSC). PTH publishes with the permission of the Chief Executive Officer, Geoscience Australia. Gary Greene, Kristin Rohr, Roy Hyndman and the editors of Geo-Marine Letters provided valuable discussion on the findings of this research.

References

Arrowsmith JR, Zielke O (2009) Tectonic geomorphology of the San Andreas Fault zone from high resolution topography: an example from the Cholame segment. Geomorphology 113:70–81

Barrie JV, Conway KW (1999) Late Quaternary glaciation and postglacial stratigraphy of the northern Pacific margin of Canada. Quat Res 51:113–123

Barrie JV, Conway KW (2002) Rapid sea level changes and coastal evolution on the Pacific margin of Canada. J Sed Geol 150:171–183

Blaise B, Clague JJ, Mathewes RW (1990) Time of maximum Late Wisconsin glaciation, west coast of Canada. Quat Res 34:282–295

Bostwick TK (1984) A re-examination of the 1949 Queen Charlotte earthquake. Dissertation, University of British Columbia

Bufe CG (2005) Stress distribution along the Fairweather-Queen Charlotte transform fault system. Bull Seismol Soc Am 95:2001–2008

Bustin AMM, Hyndman RD, Kao H, Cassidy JF (2007) Evidence for underthrusting beneath the Queen Charlotte Margin, British Columbia, from teleseismic receiver function analysis. Geophys J Int 171:1198–1211

Carlson PR, Bruns TR, Plafker G (1988) Late Cenozoic offsets on the offshore connection between the Fairweather and Queen Charlotte Faults off Southeast Alaska. Mar Geol 85:89–97

Gökaşan E, Görüm T, Tur H, Batuk F (2012) Morpho-tectonic evolution of the Çanakkale Basin (NW Anatolia): evidence for a recent tectonic inversion from transpression to transtension. Geo-Mar Lett 32(3):227–239. doi:10.1007/s00367-011-0262-y

Greene HG, Maher NM, Paull CK (2002) Physiography of the Monterey Bay National Marine Sanctuary and implications about continental margin development. Mar Geol 181:55–82

Hanson KL, Lettis WR, McLaren MK, Savage WU, Hall T (2004) Style and rate of Quaternary deformation of the Hosgri Fault Zone, offshore south-central California. In: Keller A (ed) Evolution of sedimentary basins/offshore oil and gas investigations - Santa Maria Province. US Geol Surv Bull 1995-BB

Hetherington R, Barrie JV (2004) Interaction between local tectonics and glacial unloading on the Pacific margin of Canada. Quat Int 120:65–77

Hyndman RD, Ellis RM (1981) Queen Charlotte fault zone: microearthquakes from a temporary array of land stations and ocean bottom seismographs. Can J Earth Sci 18:776–788

Hyndman RD, Hamilton TS (1993) Queen Charlotte area Cenozoic tectonics and volcanism and their association with relative plate motions along the northeastern Pacific margin. J Geophys Res 98:14257–14277

İşcan Y, Tur H, Gökaşan E (2013) Morphologic and seismic features of the Gulf of Gökova, SW Anatolia: evidence of strike-slip faulting with compression in the Aegean extensional regime. Geo-Mar Lett 33(1):31–48. doi:10.1007/s00367-012-0307-x

Johnson SY, Watt JT (2012) Influence of fault trend, bends and convergence on shallow structure and geomorphology of the Hosgri strike-slip fault, offshore central California. Geosphere 8:1632–1656

Mazzotti S, Hyndman RD, Fluck P, Smith AJ, Schmidt M (2003) Distribution of the Pacific-North America motion in the Queen Charlotte Islands-S. Alaska plate boundary zone. Geophys Res Lett 30:1762

Plafker G, Hudson T, Bruns T, Rubin M (1978) Late Quaternary offsets along the Fairweather fault and crustal plate interactions in southern Alaska. Can J Earth Sci 15:805–816

Prims J, Furlong KP, Rohr KMM, Govers R (1997) Lithospheric structure along the Queen Charlotte margin in western Canada: constraints from flexural modeling. Geo-Mar Lett 17(1):94–99. doi:10.1007/s003670050013

Rogers GC (1986) Seismic gaps along the Queen Charlotte Fault. Earthq Prediction Res 4:1–11

Rohr KMM, Tryon AJ (2010) Pacific-North America plate boundary reorganization in response to a change in relative plate motion: offshore Canada. Geochem Geophys Geosyst 11, Q06007. doi:10.1029/2009GC003019

Rohr KMM, Scheidhauer M, Trehu AM (2000) Transpression between two warm mafic plates: the Queen Charlotte Fault revisited. J Geophys Res 105:8147–8172

Shepard FP (1949) Terrestrial topography of submarine canyons revealed by diving. Geol Soc Am Bull 60:1597–1612

Smith AJ, Hyndman RD, Wang K, Cassidy JF (1993) Structure, seismicity, and thermal regime of the Queen Charlotte transform margin. J Geophys Res 108:1–12. doi:10.1029/202JB002247

Szelica W (2013) 2012 Haida Gwaii quake: insight into Cascadia's subduction extent. Eos 94:85–86

Wentworth CK (1922) A scale of grade and class terms for clastic sediments. J Geol 30:377–392